Oblique slip, slip partitioning, spatial and temporal changes in the regional stress field, and the relative strength of active faults in the Basin and Range, western United States

Steven G. Wesnousky   Center for Neotectonic Studies and Department of Geological Sciences, University of Nevada, Reno, Nevada 89557-0135

Craig H. Jones   Cooperative Institute for Research in Environmental Sciences, University of Colorado, Boulder, Colorado 80309-0216

ABSTRACT

When viewed with stress transformation laws and an idealized physical model, observations of oblique slip and slip partitioning in the Basin and Range (western United States) are interpreted to show that (1) separate regions with the same net extension direction are not necessarily characterized by the same regional stress field, (2) fault systems exhibiting partitioning where one of the faults is near vertical generally do not require temporal changes in the stress field to explain the disparate slip vectors on the adjacent faults, and (3) the relative strengths of active fault zones may vary by more than an order of magnitude.

INTRODUCTION

The purpose of this note is to illustrate how observations of oblique slip and slip partitioning on major faults in the Basin and Range, when viewed with simple stress transformation laws and an idealized physical model, can provide insight into (1) spatial and temporal variations in the regional stress field, (2) the relative strength of active faults, (3) the mechanics of low-angle faulting, and (4) the pitfall in assuming that principal stress directions determined from fault-motion indicators, such as focal-mechanism or slickenside data, are the same orientation as the principal directions of crustal strain, particularly in regions of slip partitioning. Toward that end, we limit our attention to four active faults (Table 1 and Fig. 1): the Owens Valley and Independence faults of southeast California, the 1954 Fairview Peak earthquake rupture in central Nevada, and the northern Panamint Valley low-angle normal fault also in southeastern California.

PHYSICAL FRAMEWORK

Our discussion is based on the development of two separate parameters. The development of each assumes a stress field where one of the principal stresses is oriented in the vertical.

Applying laws of stress transformation and the assumption that slip vectors on any individual active fault will parallel the shear stress resolved on the fault plane, we define the first parameter, the ratio of principal stresses,

$$S \equiv \frac{\sigma_H - \sigma_z}{\sigma_H - \sigma_h} = \sin^2 \xi + \frac{\sin 2\xi}{2 \tan \psi \, \cos^2 \Delta}, \tag{1}$$

where ψ and Δ are the slip azimuth and dip of the fault plane, respectively, σ_h is the minimum horizontal stress, σ_z is the vertical principal stress, and ξ is the angle between the maximum principal horizontal stress σ_H and the strike of the fault (Jones and Wesnousky, 1992). The relation indicates that

there is a stress field for any value of ξ that will satisfy the requirement that the shear stress resolved on the fault parallels the observed slip vector and is a specific case of more generalized results put forth previously (Angelier, 1984; Gephart and Forsyth, 1984; Michael, 1987). Values of $S > 1$ are equivalent to $\sigma_z = \sigma_3$ (reverse faulting), $0 < S < 1$ to $\sigma_z = \sigma_2$ (strike-slip faulting), and $S < 0$ to $\sigma_z = \sigma_1$ (normal faulting), where σ_1 is the most compressive principal stress.

The second parameter arises from interpretation of the idealized physical model shown in Figure 2. If the dipping fault in Figure 2 existed in the absence of the strike-slip fault (no partitioning), the slip azimuth ψ on the dipping fault would parallel the direction of oblique extension θ. When θ surpasses a certain critical angle, it becomes energetically favorable to partition a portion of the oblique component of extension onto an adjacent and parallel strike-slip fault, at which point ψ becomes $\leq \theta$. If partitioning exists, one may apply (1) a least-work criterion (Beck, 1991; Jones and Wesnousky, 1992), (2) a force-balance criterion (McCaffrey, 1992), or, with the continued assumption that slip vectors on faults parallel the shear stress resolved on the faults, and (3) simple stress transformation laws (Jones and Wesnousky, 1992) to the simplified model of Figure 1 and arrive at the relation

$$R \equiv \frac{\tau_s}{\tau_d} = \frac{\sin \psi}{\sin \Delta (1 + \cos^2\psi \, \tan^2\Delta)^{1/2}}, \tag{2}$$

where R is the ratio of shear resistance between the strike-slip (τ_s) and dipping fault (τ_d) and the remaining variables are defined in Figure 2. The relation indicates that when partitioning exists, the slip azimuth ψ is not controlled by the obliquity of extension θ but, rather, by the fault dip Δ and shear-resistance ratio R (Fig. 3). If all fault systems were characterized by the same shear resistance, the relation between ψ and Δ would follow the curve $R = 1$. More important to this analysis, equation 2 provides a tool to place bounds on the relative strengths of paired fault systems from field observations of fault dip and slip azimuth. Equation 2

TABLE 1. FAULT PARAMETERS

Fault	Reference*	Strike (°)	Dip Δ (°)	Rake† λ (°)	Slip azimuth § Ψ (°)	from north (°)
Owens Valley	1	340	85 ± 10**	-180	90	340
Independence	1,2	340	60 ± 10	-90 to -105††	0 - 38	250 - 288
Fairview Peak	3	350 ± 5	60 ± 5	-160 ± 5	75 - 83	335 - 343
Northern Panamint	4	150 ± 5	7.5 ± 7.5	-155 ± 5	70 - 80	300 - 310

*1-Beanland and Clark (1993a,b), 2-Clark et al. (1984), 3-Doser (1986); 4-Burchfiel et al. (1987).

† Conventions according to Aki and Richards (1980).

§ Slip azimuth Ψ = 90° -tan $^{-1}$ [tan(λ)cos(Δ)] (Fig. 2). Value converted to geographic coordinates in right-hand column.

** Assumed 90° when interpreted within the framework of partitioned slip; these values used in Figure 4.

†† Generally considered a normal fault, the possibility of small lateral component (rake = -105°) is assumed for illustrative purposes in this paper. Available observations do not rule out a small lateral component of slip to the system.

Figure 1. Map of active faults in western Basin and Range showing location of fault zones discussed in text (thick solid lines). Block diagram illustrates partitioning of dip-slip and strike-slip motion between Independence and Owens Valley faults, respectively.
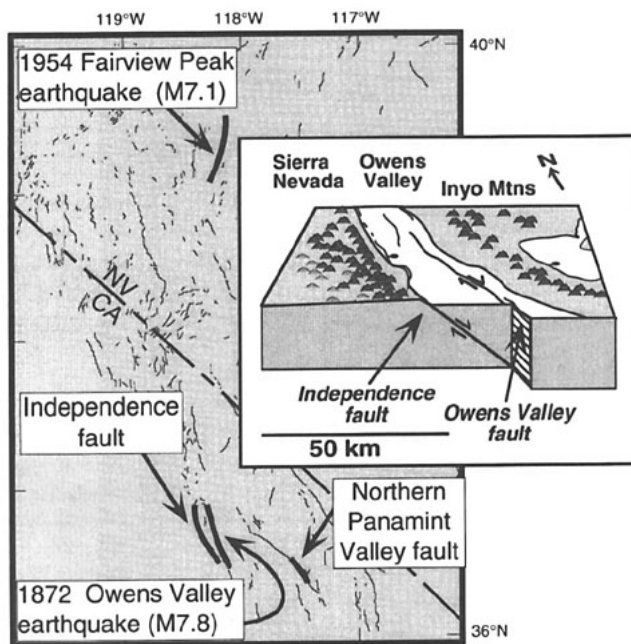
may also be applied to dipping oblique-slip faults that are not paralleled by an active strike-slip fault. In this instance, an estimate of R derived from measures of ψ and Δ on the dipping fault will necessarily be a minimum value (it is minimum because the lack of partitioning indicates that ψ is below the critical value for partitioning) and reflects only the minimum ratio of the strength of unbroken rock (in a vertical plane parallel to the dipping fault) to the dipping fault. Although currently limited to elastic or rigid blocks in the two-dimensional geometry of Figure 2 (McCaffrey, 1994), the model provides a useful framework for examining oblique and partitioned slip in the Basin and Range.

EXAMPLES FROM THE BASIN AND RANGE
Spatial Variations in Regional Stress Field
The faults indicated in Figure 1 exhibit contrasting fault geometries and slip-vector

orientations (Table 1). We can use equation 1 to examine whether there exists a single value of both S and the orientation of the principal stress directions that is compatible with the observed slip on the separate fault systems. Figure 4 is a plot of the stress ratios S that will produce the observed slip on the Independence, Fairview Peak, and Panamint Valley faults for different azimuths of least compressive horizontal stress. To satisfy the hypothesis that slip on each fault may be explained by a single stress field, the curves must intersect at a single point. Such is not the case. Hence, no single stress field explains the sense of slip observed on the faults. For example, the intersection of curves for the Independence and Panamint faults at values of $S \simeq 0.8$ indicates that they may be explained by the same stress field with a principal horizontal stress direction of about 250°. But the same stress field cannot explain observed displacements on the Fairview Peak fault. The example shows how

knowledge of fault geometries and slip vectors can place limits on possible variations in regional stress fields across the Basin and Range and supports the presence of lateral variations in stress fields akin to (but not necessarily identical to) those inferred by Zoback (1989).

Temporal Changes in Regional Stress Field
The phenomenon of slip partitioning is well exhibited by the subparallel right-lateral Owens Valley and dip-slip Independence faults in southeastern California (Fig. 1). It has been suggested that either the orientation or relative magnitudes of the principal axes of the stress field must change significantly over periods of time, on the order of multiple earthquake cycles, to explain the coexistence of the active high-angle dipslip Independence fault and the Owens Valley strike-slip fault (Zoback, 1989). We examine the hypothesis in Figure 5 by using equation 1 to plot the slip azimuth ψ vs. dip Δ for constant values of S and the minimum principal stress orientation of N80°W assumed by Zoback (1989). The lack of sensitivity of S to estimates of fault dip for near-vertical faults is illustrated by the merging of S lines at values of dip greater than about 80°. We also plot in Figure 5 the dips Δ and slip azimuths ψ for the two faults. For comparison with Zoback (1989), we allow dip on the Owens Valley fault to range between 80° and 90°. Clearly, any value of $S < 0$ can satisfy observed slip on the Owens Valley fault if the dip is vertical. The shaded region of S values for the Independence fault reflects a range of rake values between −90° and −105°. Because of the extreme sensitivity of determinations of S to fault geometry and slip azimuth for both faults and the observation that curves of constant S of $<\sim 2$ pass through the uncertainties for both fault zones, we assert that the available data are not sufficient to argue strongly that temporal
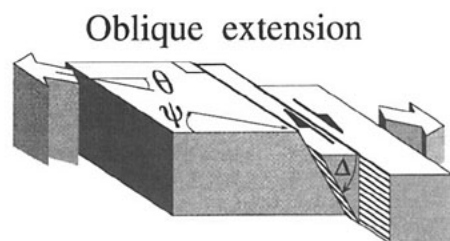

Figure 2. Oblique convergence or extension oriented at angle θ may be accommodated by slip partitioning: combination of oblique dip-slip motion on dipping fault plane (dip = Δ) and strike-slip motion on adjacent vertical fault plane. Slip azimuth ψ for dipping fault is generally less than θ in fault systems characterized by partitioning. Both θ and ψ are measured with respect to normal to fault strike.
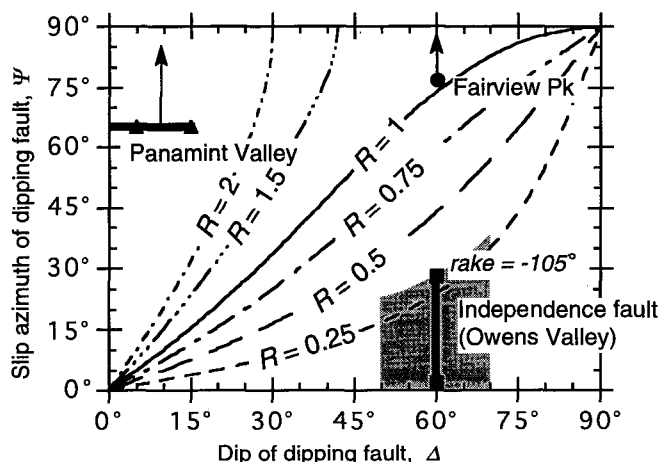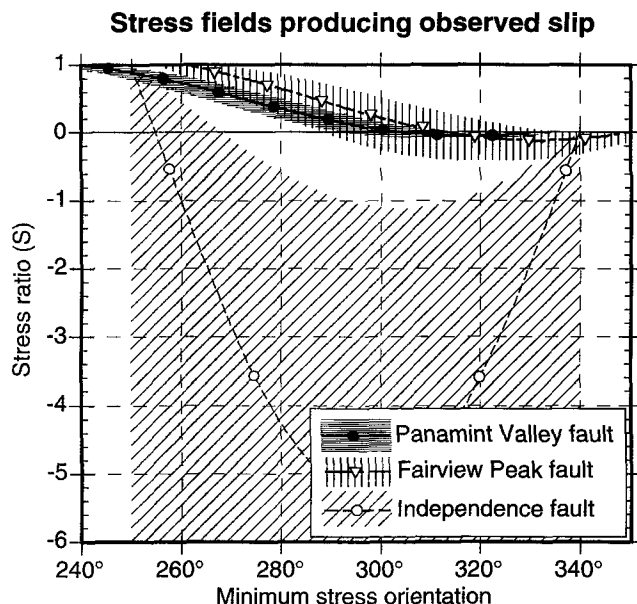

Figure 3. Contours of constant values of R computed with equation 2 on plot of dip angle Δ vs. observed slip azimuth ψ on dipping fault. Observed values of Δ and ψ indicate that R for Panamint Valley, Fairview Peak, and Independence faults range over more than an order of magnitude. See text for discussion of uncertainties (arrows and shaded area).

Figure 4. Ratio of principal stresses S determined from equation 1 vs. assumed azimuth of principal minimum-compressive horizontal stress. Lines represent computed values of S for known geometries and slip azimuths of Independence, Fairview Peak, and Panamint Valley faults. Crossings of lines indicate where slip on respective faults may be explained by a common stress field. Patterned areas show uncertainties in estimates of S arising from uncertainties in fault parameters (Table 1). Owens Valley fault not shown because strike slip on a vertical fault can be explained by any value of S.

Stress fields producing observed slip

Panamint Valley fault
Fairview Peak fault
Independence fault

Minimum stress orientation

variations in the stress ratio S are needed to explain the different mechanisms and geometries of the Independence and Owens Valley faults. Rather, an equally viable and simpler hypothesis is that, within the uncertainties, the slips on the faults are produced by the same stress field. The result is not sensitive to the assumed direction of minimum horizontal principal stress, and we may further generalize that fault systems exhibiting partitioning where one of the faults is near vertical do not generally require tem-

Figure 5. Constant values of stress ratio S computed with equation 1 are placed on plot of slip azimuth ψ vs. dip angle Δ. Values of S for Owens Valley and Independence faults are determined with values of fault dip and slip azimuth listed in Table 1. Shaded region indicates uncertainty for Independence fault, reflecting dependence of ψ on Δ. Curves for a constant stress ratio of S < ~−2 pass through uncertainties for both fault zones, indicating that slip on both faults may be explained by a single stress field.

poral changes in the stress field to explain the disparate slip vectors on the adjacent faults.

Stress vs. Strain and the Use of Focal-Mechanism and Slickenside Data in Tectonic Analysis

We observed that slip on the Owens Valley and Independence faults may be described with the same regional stress field (Fig. 5), but the slip azimuths of 250° and 340° for the Independence and Owens faults, respectively, are very different (Table 1). Therefore, the observation that the stress field across two faults is the same does not require that the slip azimuth across each fault also be the same. Similarly, if the net extension direction across two regions is the same, it is not required that the stress field across the two regions be the same. For example, if we consider that the slip rate on the Independence fault is one tenth or less that along the Owens Valley fault (Beanland and Clark 1993a, 1993b; Clark et al., 1984), the net displacement vector summed across Owens Valley and Independence faults is better defined at ~334°–340°. The value can be compared to the net extension direction of between 337° and 342° indicated by the focal mechanism of the 1954 Fairview Peak earthquake to the north in central Nevada, which occurred on a fault not characterized by partitioning. The similarity of displacement vectors for the Owens Valley and Fairview Peak regions indicates that the two regions probably share the same net extension direction. Prior tectonic analyses of focal-mechanism and slickenside data indicate that the least horizontal principal stress direction ranges between about 245° and 310° across the two regions (e.g., Zoback, 1989;
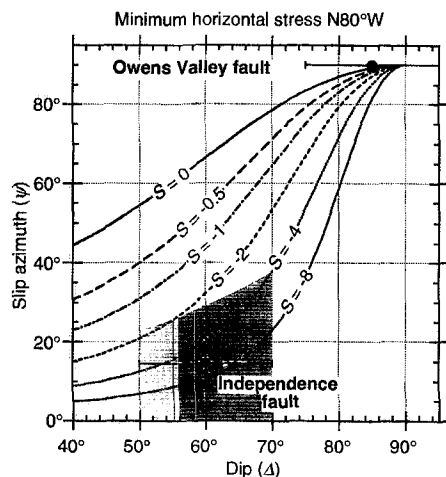
Reches, 1987). If we limit our attention in Figure 4 to this latter range of stress orientations, we observe that slip on the Fairview and Independence faults cannot be explained by a common stress field. The result illustrates the potential pitfall in assuming that principal stress directions inverted solely from collections of slickensides or focal mechanisms necessarily reflect the principal directions of crustal strain, particularly in regions of slip partitioning. It is interesting that, if we allow the possibility that minimum principal stress directions are not limited to between 245° and 310°, examination of Figure 4 allows an alternative hypothesis that the two regions do share a common stress field with $S \simeq -0.2$ and the minimum stress oriented about 337°, a direction approximately parallel to the calculated directions of extension in the two regions.

Variations in the Strength of Active Faults and the Mechanics of Low-Angle Normal Faults

The mechanics of low-angle normal faulting is a topic of considerable discussion (e.g., Buck, 1990; Forsyth, 1992). However, observations that bear directly on the physics of such faulting are rare, though several instances of active (post-Miocene to possibly Holocene) low-angle faulting have been inferred (e.g., Johnson and Loy, 1992; Burchfiel et al., 1987; MIT 1985 Field Geophysics Course and Biehler, 1987; Scott and Lister, 1992). We may use equation 2 to take advantage of information bearing on the oblique component of slip to constrain the strength of any low-angle fault relative to either an adjacent strike-slip fault or unruptured rock and, hence, provide observational constraints for physical models attempting to explain the occurrence of slip on low-angle normal faults. Entering the observed values of fault dip and slip azimuth for the Panamint Valley low-angle normal fault (Table 1) into equation 2 yields a minimum estimate of ≥ 3 for the shear-resistance ratio R (Fig. 3). Thus we infer that the Panamint Valley can be no more than 1/3 the strength ($R \geq 3$) of unbroken rock. The same approach estimates the shear-resistance ratio R to be ≥ 1 for Fairview Peak. In contrast, an estimate of R for the Owens Valley–Independence fault system yields values of R that are possibly more than an order of magnitude less than observed for either the Fairview Peak or Panamint Valley faults (Fig. 3). It is possible that the northern Panamint Valley fault also partitions slip with the Owens Valley fault (Fig. 6). If so, the shear resistance of the Panamint Valley fault is at least three times less than that of the Owens Valley fault. Therefore, the low-angle normal fault in Panamint Valley may
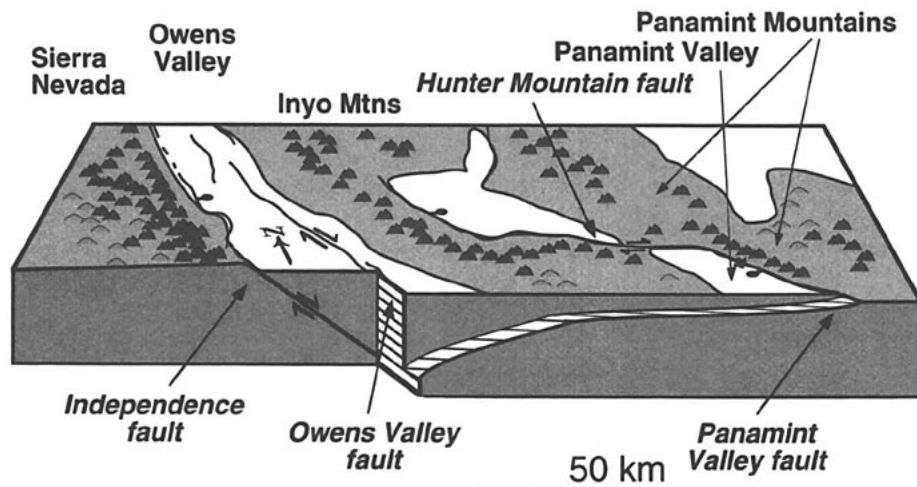
Figure 6. Shallow dip of northern Panamint Valley fault allows speculation that slip is also partitioned between Panamint Valley and Owens Valley fault zones.

have an apparent strength perhaps an order of magnitude less than that of the Independence fault. In the absence of partitioning, the large oblique component of slip on the northern Panamint Valley fault in itself still seems to require the fault to be very weak. For example, even if we were to relax our model assumptions (e.g., Spencer and Chase, 1989; Yin, 1989) to allow rotation of the stress field out of the vertical, it is difficult to reconcile a large component of oblique slip on a low-angle normal fault unless the fault is very weak; otherwise, it would partition the oblique component of slip onto a vertical strike-slip fault.

The large range in strength ratios R observed across these Basin and Range faults differs greatly from the more uniform strengths of faults found along the transpressive San Andreas fault system (Jones and Wesnousky, 1992). The apparent strength of the Independence fault might reflect the inability of the Independence fault to absorb additional extension because of the large topographic relief and, therefore, vertical component of displacement that has already been accommodated across the fault. Such an inference would be in line with the suggestion by Forsyth (1992) that high-angle normal faults become energetically less favorable with increasing amounts of extension.

SUMMARY AND CONCLUSIONS

We have presented an idealized physical framework to view the phenomena of oblique slip and slip partitioning in the Basin and Range. When considering the results in the context of the entire Basin and Range, the use of the framework serves to illustrate that (1) the relative strengths of active fault zones may vary by more than an order of magnitude, (2) separate regions exhibiting

slip partitioning and the same net extension direction are not necessarily characterized by the same regional stress field, and (3) fault systems exhibiting partitioning where one of the faults is near vertical do not generally require temporal changes in the stress field to explain the disparate slip vectors on the adjacent faults.

ACKNOWLEDGMENTS

REFERENCES CITED

Aki, K., and Richards, P. G., 1980, Quantitative seismology: Volume 1, Theory and methods: San Francisco, W. H. Freeman and Company, 558 p.
Angelier, J., 1984, Tectonic analysis of fault slip data sets: Journal of Geophysical Research, v. 89, p. 5835–5848.
Beanland, S., and Clark, M., 1993a, Late Quaternary history of the Owens Valley fault zone, eastern California, and surface rupture associated with the 1872 earthquake: Geological Society of America Abstracts with Programs, v. 25, no. 5, p. 7.
Beanland, S., and Clark, M., 1993b, The Owens Valley fault zone, eastern California, and surface rupture associated with the 1872 earthquake: U.S. Geological Survey Bulletin 1982, 29 p.
Beck, M., 1991, Coastwise transport reconsidered: Lateral displacements in oblique subduction zones, and tectonic consequences: Physics of the Earth and Planetary Interiors, v. 68, p. 1–8.
Buck, W. R., 1990, Comment on "Origin of regional, rooted low-angle normal faults—A mechanical model and its tectonic implications" by An Yin: Tectonics, v. 9, p. 545–546.
Burchfiel, B. C., Hodges, K. V., and Royden, L. H., 1987, Geology of Panamint Valley–Saline Valley pull-apart system, California: Palinspastic evidence for low-angle geom-

etry of a Neogene range-bounding fault: Journal of Geophysical Research, v. 92, p. 10,422–10,426.
Clark, M. M., and 11 others, 1984, Preliminary slip rate tables for late Quaternary faults of California: U.S. Geological Survey Open-File Report 84-106, 12 p.
Doser, D. I., 1986, Earthquake processes in the Rainbow Mountain–Fairview Peak–Dixie Valley, Nevada, region 1954–1959: Journal of Geophysical Research, v. 91, p. 12,572–12,586.
Forsyth, D. W., 1992, Finite extension and low-angle normal faulting: Geology, v. 20, p. 27–30.
Gephart, J. W., and Forsyth, D. W., 1984, An improved method for determining the regional stress tensor using earthquake focal mechanism data: Application to the San Fernando earthquake sequence: Journal of Geophysical Research, v. 89, p. 9305–9320.
Johnson, R. A., and Loy, K. L., 1992, Seismic reflection evidence of seismogenic low-angle faulting in southeastern Arizona: Geology, v. 20, p. 597–600.
Jones, C. H., and Wesnousky, S. G., 1992, Variations in strength and slip rate along the San Andreas Fault system: Science, v. 256, p. 83–86.
McCaffrey, R., 1992, Oblique plate convergence, slip vectors, and forearc deformation: Journal of Geophysical Research, v. 97, p. 8905–8915.
McCaffrey, R., 1994, Global variability in subduction thrust zone–forearc systems: Pure and Applied Geophysics, v. 142, p. 173–224.
Michael, A. J., 1987, The use of focal mechanisms to determine stress: A control study: Journal of Geophysical Research, v. 92, p. 357–368.
MIT 1985 Field Geophysics Course and Biehler, S., 1987, A geophysical investigation of the northern Panamint Valley, Inyo County, California: Evidence for possible low-angle normal faulting at shallow depth in the crust: Journal of Geophysical Research, v. 92, p. 10,427–10,441.
Reches, Z., 1987, Determination of the tectonic stress tensor from slip along faults that obey the Coulomb yield condition: Tectonics, v. 6, p. 849–861.
Scott, R. J., and Lister, G. S., 1992, Detachment faults; evidence for a low-angle origin: Geology, v. 20, p. 833–836.
Spencer, J. E., and Chase, C. G., 1989, Role of crustal flexure in initiation of low-angle normal faults and implications for structural evolution of the Basin and Range province: Journal of Geophysical Research, v. 94, p. 1765–1775.
Yin, A., 1989, Origin of regional, rooted low-angle normal faults—A mechanical model and its tectonic implications: Tectonics, v. 8, p. 469–482.
Zoback, M. L., 1989, State of stress and modern deformation of the northern Basin and Range province: Journal of Geophysical Research, v. 94, p. 7105–7128.

Printed in U.S.A.